3.9.5

$^{6}Li/^{7}Li$ and $^{14}N/^{15}N$ isotopic substitution experiments using NOVA spectrometer at J-PARC

Yasuo Kameda*[1], Takuya Miyazaki[1], Yuko Amo[1], Takeshi Usuki[1] and Toshiya Otomo[2]
[1]Department of Material and Biological Chemistry, Faculty of Science, Yamagata University, Yamagata 990-8560, Japan
[2]Institute of Material Structure Science, KEK, Tsukuba, Ibaraki 305-0801, Japan

E-mail: kameda@sci.kj.yamagata-u.ac.jp

Abstract. Neutron scattering measurements have been carried out for $^{6}Li/^{7}Li$ and $^{14}N/^{15}N$ isotopically substituted aqueous $^{*}Li^{*}NO_3$ solutions in D_2O using the high intensity total scattering spectrometer NOVA installed in J-PARC. In the present study, concentration of the solute was extended to the very dilute region at 1 mol% $LiNO_3$, and information on the hydration structure of Li^+ and NO_3^- was successfully deduced. In the aqueous 1 mol% $LiNO_3$ solution, it has been found that Li^+ is surrounded by 6.0 ± 0.2 water molecules with the nearest neighbour $Li^{+}\cdots O$ distance of 2.00 ± 0.02 Å. The hydration number of NO_3^- in aqueous 1 mol% $LiNO_3$ solution is determined to be 6 ± 2 with the intermolecular distance between N atom and the nearest neighbour D (D_2O) atom of 3.0 ± 0.1 Å. Concentration dependence of hydration parameters for these ions is discussed.

1. Introduction

Isotopic substitution method is one of the most promising applications in the structural investigations of non-crystalline materials using neutron total scattering experiments. The environmental structure around isotopically substituted atom can be extracted by taking subtraction of scattering cross sections observed for samples with different isotopic compositions [1]. A drawback of this technique might be the difficulty in obtaining sufficient S/N ratio of subtracted intensity data. In order to keep favourable statistical accuracy in the subtracted intensity, the use of high intensity incident neutron beam is indispensable.

In the present paper, we report results of neutron scattering measurements on $^{6}Li/^{7}Li$ and $^{14}N/^{15}N$ substituted aqueous $^{*}Li^{*}NO_3$ solutions in D_2O using the NOVA spectrometer installed in J-PARC. In the present study, concentration of the solute was extended to the very dilute region at 1 mol% $LiNO_3$ and information on the hydration structure of Li^+ and NO_3^- was successfully deduced. In the present analysis, the re-normalization procedure for the observed scattering cross sections was applied employing the least squares fitting analysis of intramolecular interference terms for D_2O and NO_3^- in order to confirm the absolute amplitude of observed difference function.

*To whom any correspondence should be addressed.

2. Experimental and Data Analysis

^{6}Li- and ^{7}Li-enriched lithium nitrate was prepared by reacting $^{6}Li_2CO_3$ (95.6% ^{6}Li) and $^{7}LiOH{\cdot}H_2O$ (99.94% ^{7}Li) with slightly excess amount of concentrated $H^{14}NO_3$ (99.6% ^{14}N, natural abundance) and $H^{15}NO_3$ (88.9% ^{15}N) aqueous solutions. The dehydration of the product solution was achieved by heating at 180 ºC under vacuum more than a day. The weighted amount of enriched anhydrous $^{*}Li^{*}NO_3$ was dissolved into D_2O (99.9 % D, Aldrich Chemical Co.) to prepare 1, 5 and 10 mol% $^{*}Li^{*}NO_3$ solutions with different ^{6}Li/^{7}Li and ^{14}N/^{15}N isotopic compositions. Average coherent scattering lengths of Li and N atoms in sample solutions used in this study are summarized in Table 1. The sample solution was introduced into a thin-walled cylindrical vanadium cell (6.0 mm in inner diameter and 0.1 mm in thickness) and sealed by an Indium-seal.

Table 1. Average coherent scattering lengths of Li and N atoms.

Sample	$b_{Li}/10^{-12}$cm	$b_{N}/10^{-12}$cm
$(^{6}Li^{14}NO_3)_{0.1}(D_2O)_{0.9}$	0.182	0.936
$(^{7}Li^{14}NO_3)_{0.1}(D_2O)_{0.9}$	-0.222	0.936
$(^{7}Li^{15}NO_3)_{0.1}(D_2O)_{0.9}$	-0.222	0.677
$(^{6}Li^{14}NO_3)_{0.05}(D_2O)_{0.95}$	0.182	0.936
$(^{7}Li^{14}NO_3)_{0.05}(D_2O)_{0.95}$	-0.222	0.936
$(^{7}Li^{15}NO_3)_{0.05}(D_2O)_{0.95}$	-0.222	0.677
$(^{6}Li^{14}NO_3)_{0.01}(D_2O)_{0.99}$	0.182	0.936
$(^{7}Li^{14}NO_3)_{0.01}(D_2O)_{0.99}$	-0.222	0.936
$(^{7}Li^{15}NO_3)_{0.01}(D_2O)_{0.99}$	-0.222	0.677

Neutron diffraction measurements were carried out at 25 ºC using the NOVA spectrometer [2] installed at BL21 of the MLF pulsed neutron source in the J-PARC, Tokai, Japan. Incident proton beam power of proton accelerator was 160 kW in measurements for 5 and 10 mol% $^{*}Li^{*}NO_3$ solutions, and 220 kW for 1 mol% $^{*}Li^{*}NO_3$ solutions, respectively. Scattered neutrons (neutron wave band of $0.1 \leq \lambda \leq 8.7$ Å) were detected by ca. 900 of 20 atm ^{3}He position sensitive proportional counters (1/2 inch ϕ, 800 mm in active length with 5 mm in positional resolution) installed at 20º (13.1 – 27.9º), 45º (33.6 – 54.9º), 90º (72.7 – 107.4º) and back scattering (136.5 – 169.0º) detector banks. Data accumulation time was ca. 4 h for each sample. Measurements were made in advance for 6 mm ϕ vanadium rod, empty cell and instrumental background.

Observed scattering intensities for the sample were corrected for instrumental background, absorption of sample and cell [3], multiple [4] and incoherent scatterings. The coherent scattering lengths, scattering and absorption cross sections for the constituent nuclei were referred to those tabulated by Sears [5]. The wavelength dependence of the total cross sections for H and D nuclei was estimated from the observed total cross sections for H_2O and D_2O, respectively [6]. The inelasticity correction for the observed self-scattering term was applied by the use of the observed self-scattering intensities from the liquid null-H_2O [7].

The first-order difference function $\Delta_X(Q)$, X = Li and N, is derived from the numerical difference between scattering cross sections observed for two solutions that are identical except for the scattering lengths of Li or N atoms [1]. The $\Delta_X(Q)$ normalized for a stoichiometric unit, $(^{*}Li^{*}NO_3)_x(D_2O)_{1-x}$, can be written as a linear combination of partial structure factors, $a_{Xj}(Q)$, involving contributions from the X-j pair:

$$\Delta_X(Q) = \Sigma A_{Xj}[a_{Xj}(Q) - 1]. \quad (1)$$

The weighting of the structure factor can be written as $A_{Xj} = 2c_X c_j \Delta b_X b_j$ (for j ≠ X) and $A_{Xj} = c_X^2(b_X^2 - b_{X'}^2)$ (for j = X), where c_j and b_j denote the number in the stoichiometric unit and the coherent scattering length of j atom, respectively. Since the weighting factors, A_{XO} and A_{XD} are much

larger than others in the present experimental condition, the observed $\Delta_X(Q)$ is dominated by the short-range X-D_2O interaction. The observed $\Delta_X(Q)$ from forward angle detector pixels located at $13.1 \leq 2\theta \leq 54.9^o$ agree well within the statistical uncertainties, they were combined at the Q-interval of 0.1 Å^{-1} and used for subsequent analyses. The distribution function around X atom, $G_X(r)$, is obtained from the Fourier transform of $\Delta_X(Q)$:

$$G_X(r) = 1 + (\Sigma A_{Xj})^{-1}(2\pi^2\rho r)^{-1}\int_0^{Q_{max}} Q\Delta_X(Q)\sin(Qr)\,dQ$$
$$= [\Sigma A_{Xj}\, g_{Xj}(r)]\,(\Sigma A_{Xj})^{-1}, \quad (2)$$

where, ρ denotes the number density of the sample. The upper limit of the integral was set to be 20 Å^{-1} in the present study.

Structural parameters concerning the hydration shell of X were obtained through the least squares fitting procedure applying the following model function [8-10]:

$$\Delta_X^{model}(Q) = \Sigma\, 2c_X n_{X\alpha} b_\alpha \Delta b_X \exp(-l_{X\alpha}^2 Q^2/2)\sin(Qr_{X\alpha})/(Qr_{X\alpha})$$
$$+ 4\pi\rho\,(\Sigma A_{Xj})\exp(-l_0^2 Q^2/2)[Qr_0\cos(Qr_0) - \sin(Qr_0)]Q^{-3} + \gamma, \quad (3)$$

where, $n_{Li\alpha}$ is the coordination number of α atom around X. Sort-range parameters $l_{X\alpha}$ and $r_{X\alpha}$ denote the root-mean-square amplitude and internuclear distance of the X···α pair, respectively. The long-range parameter, r_0, means the distance beyond which the continuous distribution of atoms around X can be assumed. The parameter, l_0, describes the sharpness of the boundary at r_0. A constant, γ, was introduced to adjust the center of the interference oscillation, which is effective for improving the fit. Structural parameters $n_{X\alpha}$, $l_{X\alpha}$, $r_{X\alpha}$, l_0, r_0 and γ are determined from the least squares fit to the observed $\Delta_X(Q)$. The fitting procedure was performed in the range of $0.1 \leq Q \leq 20.0$ Å^{-1} with the SALS program [11], assuming that the statistical uncertainties distribute uniformly. In the least squares fitting calculation, the Marquardt method was employed. The dynamical bi-weight method was used for weight adjustment of the observed data [11].

In order to check reliability of the data correction and normalization procedures employed in the present study, the least squares fitting analysis was first carried out for the observed total interference term before taking the first-order difference. Since intermolecular interference term diminishes much faster than intramolecular one with increasing Q-value, interference amplitude observed in sufficiently high-Q region can be regarded as the intramolecular interference contribution. In the present analysis, the theoretical intramolecular interference term, $i^{intra}(Q)$, was evaluated by the sum of intramolecular interference terms for D_2O, $i_{D_2O}{}^{intra}(Q)$, and NO_3^-, $i_{NO_3^-}{}^{intra}(Q)$, molecules as follows:

$$i^{intra}(Q) = \beta[(1-x)\, i_{D_2O}{}^{intra}(Q) + x\, i_{NO_3^-}{}^{intra}(Q)], \quad (4)$$

where

$$i_{D_2O}{}^{intra}(Q) = 4b_O b_D \exp(-l_{OD}^2 Q^2/2)\sin(Qr_{OD})/(Qr_{OD})$$
$$+ 2b_D^2 \exp(-l_{DD}^2 Q^2/2)\sin(Qr_{DD})/(Qr_{DD}), \quad (5)$$

and

$$i_{NO_3^-}{}^{intra}(Q) = 6\, b_N b_O \exp(-l_{NO}^2 Q^2/2)\sin(Qr_{NO})/(Qr_{NO})$$
$$+ 6b_O^2 \exp(-l_{OO}^2 Q^2/2)\sin(Qr_{OO})/(Qr_{OO}). \quad (6)$$

β denotes the overall renormalization factor which indicates appropriateness of the data correction and normalization procedures employed. In the fitting procedure, intramolecular parameters for D_2O molecule, l_{OD}, r_{OD}, l_{DD} and r_{DD}, as well as the factor β were treated as independent parameters. Since contribution from the intramolecular interference term for NO_3^- should be relatively small, intramolecular parameters for NO_3^- were fixed to the literature values (l_{NO} = 0.045 Å, r_{NO} = 1.252 Å, l_{OO} = 0.065 Å, and r_{OO} = 2.169 Å) [12-14]. The least squares fitting analysis was performed in the range of $10 \leq Q \leq 40$ Å^{-1} with the SALS program [11].

3. Results and Discussion

Before evaluation of the first-order difference function, the least squares fitting analysis was carried out for the observed total interference function to check the absolute interference amplitude of each sample solution using equation (4). To avoid large inelasticity effect on the observed scattering intensity, scattering cross sections obtained from forward angle detector banks (13.1 – 54.9º) were combined at the Q-interval of 0.1 Å^{-1} and used for the least squares fitting analysis. A satisfactory fit was obtained in the range of $10 \leq Q \leq 40$ Å^{-1}. The value of renormalization factor, β, for each solution is very close to the unity within the experimental uncertainties (β = 0.96(2) – 1.01(3)), implying that data correction and normalization procedures have been adequately carried out in the present study and the absolute value of the difference function should be reliable. The present value of intramolecular O-D distance within D_2O (r_{OD} = 0.970 - 0.976 Å) is somewhat slightly small when compared with that reported for pure liquid water (0.983(8) Å [15], 0.983(5) Å [16], 0.987(5) Å [17]). The present values of r.m.s. amplitudes for the intramolecular O-D and D-D interactions (l_{OD} = 0.058 - 0.061 Å and l_{DD} = 0.117 – 0.14 Å) are in good agreement with those for pure liquid water (l_{OD} = 0.067(8) Å and l_{DD} = 0.12(4) Å [16]).

The first order difference function, $\Delta_{Li}(Q)$, observed for 1, 5 and 10 mol% $Li^{14}NO_3$ solutions is represented in Figure. 1. The distribution function around Li^+, $G_{Li}(r)$, was obtained from the Fourier transform of the observed $\Delta_{Li}(Q)$ as depicted in Figure. 2.

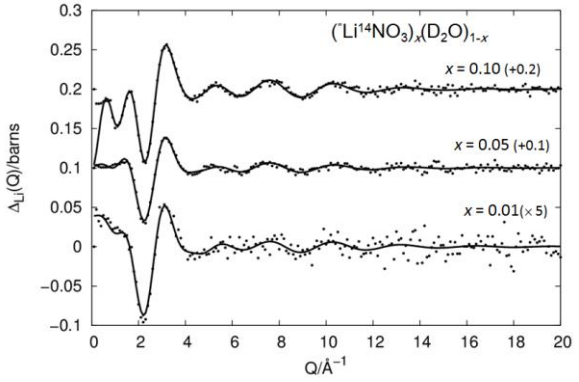

Figure 1. First-order difference function, $\Delta_{Li}(Q)$, observed for 1, 5 and 10 mol% $^*Li^{14}NO_3$ heavy water solutions (dots). The best fit of the calculated $\Delta_{Li}(Q)$ is indicated by a solid line.

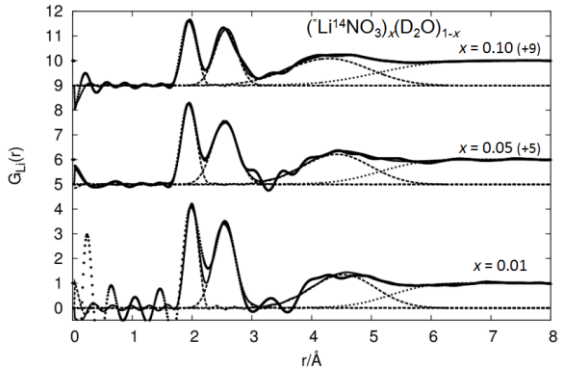

Figure 2. Distribution function around Li^+, $G_{Li}(r)$, observed for 1, 5 and 10 mol% $^*Li^{14}NO_3$ heavy water solutions (dots). The Fourier transform of the best fit of calculated $\Delta_{Li}(Q)$ is indicated by a solid line. Short- and long-range contributions are denoted by a broken- and dotted lines, respectively.

Dominant short range peaks appearing at around 2 and 2.6 Å in the present $G_{Li}(r)$, are assigned to the nearest neighbour $Li^{+}\cdots O$ and $Li^{+}\cdots D$ interactions, respectively [18-24]. In the fitting procedure, the structural parameter, n_{LiD}, was fixed to $2n_{LiO}$ during the present least squares fitting procedure. The second coordination sphere of Li^{+} was treated as a single interaction with the coherent neutron scattering length in equation (3), b_{α}, being $b_O + 2b_D$. The long-range random distribution of atoms was taken into account in the analysis, which is important to improve the fit in the low-Q region. As described in Figure. 1, the observed $\Delta_{Li}(Q)$ for each solution is satisfactorily reproduced by the calculated model function in the whole Q-range observed. Final results of independent parameters are listed in Table 2.

Table 2. Results of the least-squares refinement of the observed $\Delta_{Li}(Q)$[a].

x	interaction	i···j	r_{ij}/Å	l_{ij}/Å	n_{ij}
0.1	$Li^{+}\cdots D_2O$(I)	$Li^{+}\cdots O$	1.969(8)	0.117(9)	4.12(6)
		$Li^{+}\cdots D$	2.58(1)	0.187(7)	[6.24][b]
	$Li^{+}\cdots D_2O$(II)	$Li^{+}\cdots D_2O$	4.4(1)	0.68(2)	14(4)
			r_0/Å	l_0/Å	
	Long-range		5.2(3)	0.8(3)	
0.05	$Li^{+}\cdots D_2O$(I)	$Li^{+}\cdots O$	1.957(4)	0.113(5)	5.18(3)
		$Li^{+}\cdots D$	2.564(5)	0.204(4)	[10.36][b]
	$Li^{+}\cdots D_2O$(II)	$Li^{+}\cdots D_2O$	4.5(1)	0.563(9)	14(5)
			r_0/Å	l_0/Å	
	Long-range		5.2(4)	0.6(4)	
0.01	$Li^{+}\cdots D_2O$(I)	$Li^{+}\cdots O$	2.00(2)	0.10(3)	6.0(2)
		$Li^{+}\cdots D$	2.55(4)	0.18(2)	[12.0][b]
	$Li^{+}\cdots D_2O$(II)	$Li^{+}\cdots D_2O$	4.6(5)	0.54(4)	15(3)
			r_0/Å	l_0/Å	
	Long-range		5.4(2)	0.5(1)	

[a] Estimated standard deviations are given in parentheses.

[b] Fixed at the value $2n_{LiO}$.

The present value of r_{LiO}, for 5 and 10 mol% $LiNO_3$ solutions is in good agreement with that obtained in previous neutron diffraction studies [18-22], while, the value, r_{LiO} = 2.00(2) Å determined for 1 mol% $LiNO_3$ solution is slightly larger than those obtained for more concentrated solutions. The present values of the nearest neighbor $Li^{+}\cdots D$ distance, 2.55(4), 2.564(5) and 2.58(1) Å observed for 1, 5 and 10 mol% $LiNO_3$ solutions agree well with those reported previously [18-22]. The present results of n_{LiO} for $LiNO_3$ solutions indicate that the concentration dependence of the hydration number of Li^{+} is actually present. Previous neutron diffraction studies for aqueous LiCl [18,19] and LiBr [20] solutions suggested that hydration number of Li^{+} varies with solute concentration.

Difference functions, $\Delta_N(Q)$, observed for 1, 5 and 10 mol% $^7Li^*NO_3$ solutions are indicated in Figure 3. Interference features extended to higher-Q region are clearly observed. The distribution functions around N atom within NO_3^- are depicted in Figure 4. Dominant first peak located at r = 1.25 Å is obviously assigned to intramolecular N-O interaction within the NO_3^-. A broad peak appearing at $r \sim 3$ Å is attributable to the nearest neighbour $N\cdots D_1$ (D_2O) interaction, which has been found for concentrated aqueous $NaNO_3$ solution [13]. The nearest neighbour $N\cdots O$ (D_2O) and $N\cdots D_2$ (D_2O) interactions are certainly involved in the r-range $r = 3 \sim 4$ Å in the present $G_N(r)$ functions.

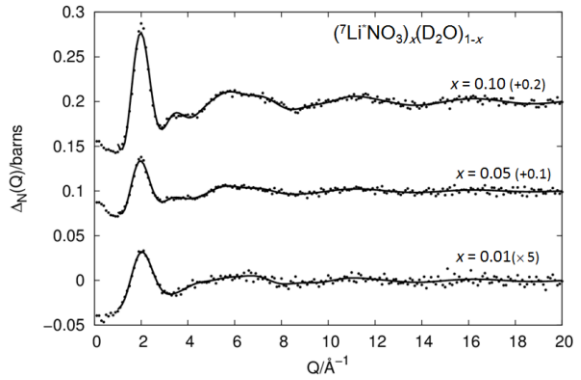

Figure 3. First-order difference function, $\Delta_N(Q)$, observed for 1, 5 and 10 mol% $^7Li^*NO_3$ heavy water solutions (dots). The best fit of the calculated $\Delta_N(Q)$ is indicated by a solid line.

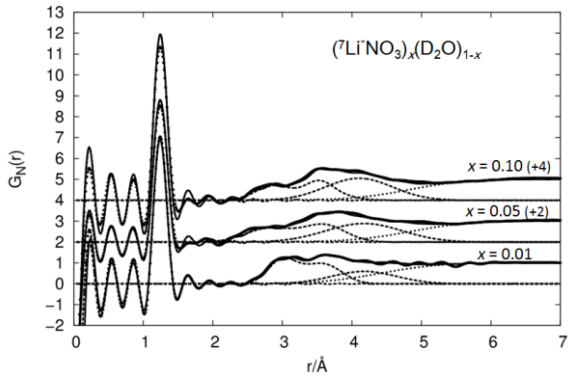

Figure 4. Distribution function around N atom, $G_N(r)$, observed for 1, 5 and 10 mol% $^7Li^*NO_3$ heavy water solutions (dots). The Fourier transform of the best fit $\Delta_N(Q)$ is indicated by a solid line. Short- and long-range contributions are denoted by a broken- and dotted lines, respectively.

Hydration parameters of NO_3^- were determined through the least squares fitting analysis of the observed $\Delta_N(Q)$. In the fitting procedure, the intramolecular N-O, the intermolecular first nearest neighbour N···D_2O(I) and the second nearest neighbour N···D_2O(II) interactions were taken into account for short-range interactions. In the fitting procedure, intramolecular parameter n_{NO} was fixed to 3 considering the intramolecular structure of NO_3^-. For the first nearest neighbour N···D_2O(I) interaction, structural parameters r_{NO}, l_{NO} and a bond angle ∠N-O···D_{w1} were treated as independent parameters. The second nearest neighbour N···D_2O(II) interaction was treated as a single interaction with the coherent scattering length b_α, being $b_O + 2b_D$. The long-range random distribution of atoms was involved in the model function. The refinement for the observed $\Delta_N(Q)$ was carried out in the range with $1.0 \le Q \le 20.0$ Å^{-1}.

Table 3. Results of the least-squares refinement of the observed $\Delta_N(Q)$[a].

x	interaction	i···j	r_{ij}/Å	l_{ij}/Å	n_{ij}
0.1	Intramolecular	N-O	1.254(1)	0.050(1)	[3.0][b]
	N···D_2O(I)	N···D_{w1}	2.90(2)	0.261(2)	4.4(3)
		∠N-O···D_{w1}	136.9(2)°		
	N···D_2O(II)	N···D_2O	4.16(2)	0.48(2)	8.8(5)
			r_0/Å	l_0/Å	
	Long-range		4.92(2)	0.64(2)	
0.05	Intramolecular	N-O	1.253(1)	0.070(1)	[3.0][b]
	N···D_2O(I)	N···D_{w1}	2.85(4)	0.329(3)	5.2(7)
		∠N-O···D_{w1}	142(4)°		
	N···D_2O(II)	N···D_2O	4.25(2)	0.55(5)	9(1)
			r_0/Å	l_0/Å	
	Long-range		4.95(4)	0.55(4)	
0.01	Intramolecular	N-O	1.250(1)	0.054(1)	[3.0][b]
	N···D_2O(I)	N···D_{w1}	3.0(1)	0.198(2)	6(2)
		∠N-O···D_{w1}	129(11)°		
	N···D_2O(II)	N···D_2O	4.2(3)	0.5(3)	6(3)
			r_0/Å	l_0/Å	
	Long-range		4.5(1)	0.68(9)	

[a] Estimated standard deviations are given in parentheses.
[b] Fixed.

The present value of intramolecular N-O distance agrees well with that observed in aqueous $NaNO_3$ solution [13] and molten $LiNO_3$ [12]. The nearest neighbour $N^{\cdots}D_{w1}$ distance was obtained to be 3.0(1), 2.85(4) and 2.90(2) Å for 1, 5 and 10 mol% $LiNO_3$ solutions. These values agree well with the value 2.8 Å reported for aqueous 10 mol% $NaNO_3$ solution [13]. The hydration number of NO_3^- is found to change from 4.4 in the 10 mol% $LiNO_3$ solution to 6 in the 1 mol% $LiNO_3$ solution.

Acknowledgements

The authors would like to thank the instrumental staff members of the NOVA spectrometer for their help during the course of neutron diffraction measurement and transformation of the scattering data. The neutron scattering experiment was approved by the Neutron Scattering Program Advisory Committee of IMSS, KEK (Proposal No. 2009S06). This work was partially supported by Grant-in-Aid for Scientific Research (C) (No. 26390110) from the Ministry of Education, Culture, Sports, Science and Technology, Japan.

References

[1] Enderby J E and Neulson G W 1979 *Water, A Comprehensive Treatise* vol 6 (Plenum press, New York and London) p 1
[2] Otomo T, Suzuya K, Misawa M, Kaneko N, Ohshita H, Fukunaga T, Itoh K, Mori K, Sugiyama M, Kameda Y, Yamaguchi T, Yoshida K, Kawakita Y, Maruyama K, Shamoto S, Takeda S, Saitoh S, Muto S, Suzuki J, Ino I, Shimizu H, Kamiyama T, Ikeda S, Yasu Y, Nakayoshi K, Senda H, Uno S and Tanaka M 2011 *MLF Annual Report 2009, J-PARC* 10-05, p 62
[3] Paalman H H and Pings C J 1962 *J. Appl. Phys.* **33** 2635
[4] Blech I A and Averbach B L 1965 *Phys. Rev.* **137** A1113
[5] Sears V F 1992 *Neutron News* **3** 26
[6] Granada J R, Gillette V H and Mayer R E 1987 *Phys. Rev. A* **36** 5594
[7] Kameda Y, Sasaki M, Usuki T, Otomo T, Itoh K, Suzuya K, Fukunaga T 2003 *J. Neutron Research* **11** 153
[8] Narten A H, Danford M D and Levy H A 1967 *Discuss. Faraday Soc*. **43** 97
[9] Caminiti R, Cucca P, Monduzzi M and Saba G 1984 *J. Chem. Phys*. **81** 543
[10] Ohtaki H, Fukushima N 1992 *J. Solution Chem*. **21** 23
[11] Nakagawa T and Oyanagi Y 1980 *Program system SALS for nonlinear least-squares fitting in experimental sciences −from Recent Developments in Statistical Inference and Data Analysis* (North-Holland, Amsterdam)
[12] Kameda Y, Kotani S and Ichikawa K 1992 *Mol. Phys*. **75** 1
[13] Kameda Y, Saitoh H and Uemura O 1993 *Bull. Chem. Soc. Jpn.* **66** 1919
[14] Kameda Y, Sugawara K, Usuki T and Uemura O 1998 *Bull. Chem. Soc. Jpn.* **71** 2769
[15] Powles J G 1981 *Mol. Phys.* **42** 757
[16] Kameda Y and Uemura O 1992 *Bull. Chem. Soc. Jpn*. **65** 2021
[17] Zeidler A, Salmon P S, Fischer H E, Neuefeind J C, Simonson J M, Lemmel H, Rauch H and Markland T 2011 *Phys. Rev. Lett*. **107** 145501-1
[18] Newsome J R, Neilson G W and Enderby J E 1980 *J. Phys. C: Solid State Phys.* **13** L923
[19] Howell I and Neilson G W 1996 *J. Phys.: Condens. Matter* **8** 4455
[20] Kameda Y, Suzuki S, Ebata H, Usuki T and Uemura O 1997 *Bull. Chem. Soc. Jpn*. **70** 42
[21] Kameda Y, Mochiduki K, Imano M, Naganuma H, Sasaki M, Amo Y and Usuki T 2005 *J. Mol. Liq*. **119** 159
[22] Kameda Y and Uemura O 1993 *Bull. Chem. Soc. Jpn.* **66** 384
[23] Yamagami M, Yamaguchi T, Wakita H and Misawa M 1994 *J. Chem. Phys.* **100** 3122
[24] Yamaguchi T, Ohzono H, Yamagami M, Yamanaka K, Yoshida K and Wakita H 2010 *J. Mol. Liq*. **153** 2